International Journal of Science and Future Technologies

Temporal Resolution of Solar Resource Data and Reliability of PV−Battery Systems: A Five-Year Multi-Climate Chronological Simulation

Morgan D. Phill [1*]
[1] PhD, Department of Renewable Energy Engineering, Oregon University, Oregon, USA

*** Corresponding Author**: morgan.dp3@oit.ed

Citation: M.D. Phill. "Temporal Resolution of Solar Resource Data and Reliability of PV− Battery Systems: A Five-Year Multi-Climate Chronological Simulation". *International Journal of Science and Future Technologies*, vol. 1, no. 1, pp. 1 – 17, 2026.

Received: 10 Jan 2026

Accepted: 04 Apr 2026

Abstract

This study quantifies how temporal treatment of solar-resource data changes the simulated reliability and storage requirements of a photovoltaic (PV)–battery system. Hourly NASA POWER data for global horizontal irradiance (GHI), 2-m air temperature, and 10-m wind speed were analyzed for Phoenix, Tucson, Atlanta, London, Munich, and Rovaniemi over 1 January 2019 to 31 December 2023. The native hourly series (H) was compared with two daily-to-hourly reconstructions: a 24-h flat reconstruction (D_flat) and a daylight-weighted sinusoidal reconstruction (D_sin). The baseline system comprised a 10-Wp PV array, a constant 2-W DC load, and a 50-Wh nominal battery, with 80% maximum depth of discharge, 85% round-trip efficiency, and 100% initial state of charge. PV output was simulated using tilted-plane irradiance, module temperature, and a PVWatts-type relation. Reliability was measured as the fraction of load-hours with unmet demand (LPSP), and nominal battery capacity was searched for 1% and 0.1% LPSP targets. Annual PV yields under H ranged from 8.55 to 20.24 kWh yr−1, while D_flat reduced yield by 12.1−38.8% relative to H. With the 50-Wh battery, LPSP under H ranged from 6.4% in Phoenix to 62.1% in Rovaniemi, whereas D_flat increased LPSP by 55−349%. In contrast, the relative LPSP difference under D_sin ranged from −5.1% to +4.2% compared with H. Friedman's test showed a significant overall treatment effect on LPSP (χ^2=9.33, p=0.0094, Kendall's W=0.78). At the 1% target, the required nominal battery capacities in Tucson and Phoenix were 592−728 Wh under H/D_sin, compared with 2.45−3.82 kWh under D_flat. The results show that preserving daily solar energy does not necessarily preserve chronological PV – battery reliability and that daylight-constrained reconstruction is substantially less biased than uniform 24-h redistribution.

Keywords: Photovoltaic-Battery System, Temporal Resolution, Nasa Power, Loss of Power Supply Probability, Battery Sizing, Solar Resource

INTRODUCTION

Photovoltaic (PV) generation is intrinsically time dependent. The same daily irradiation total can correspond to very different electrical operating trajectories depending on whether the energy arrives in a narrow daylight window, is spread smoothly through daylight hours, or is represented by a coarse average that obscures sunrise, sunset, and intraday weather structure. This distinction matters whenever generation is paired with finite storage. A battery does not respond to daily energy totals alone; it responds to the chronological sequence of surplus and deficit intervals, the state of charge (SOC), and the maximum usable storage range. Early solar-resource work established relationships among global, direct, and diffuse radiation that remain foundational for temporal reconstruction of irradiance [1], while the Erbs diffuse-fraction model provides a widely used relationship between hourly clearness index and diffuse fraction [2]. Classical PV-battery

Copyright © 2026 by Author/s. IJSFT is an open access article distributed under the Creative Commons Attribution License which permits unrestricted use, distribution, and reproduction in any medium, provided the original work is properly cited.

performance formulations also show that storage changes the relationship between solar-resource statistics and load coverage [3].

The increasing availability of satellite and reanalysis products has made hourly solar-resource data accessible at locations without long-term ground measurements. NASA POWER provides globally distributed solar and meteorological analysis-ready data, including hourly surface shortwave irradiance, air temperature, and wind speed [4]. Such datasets are attractive for preliminary PV system studies because they offer consistent spatial coverage and long records. Nevertheless, many engineering workflows still use daily or monthly data, especially at the early screening stage. A daily total is convenient for resource assessment, but its transformation into a chronological hourly profile necessarily introduces assumptions about when the radiation occurred.

The scientific problem addressed here is therefore not whether daily solar energy can reproduce annual energy totals, but whether alternative intraday reconstructions preserve the reliability characteristics of a PV–battery system. This is particularly important for small stand-alone systems, where the battery is the only buffer between a variable source and a continuous load. Chronological simulations can identify the exact hours in which the battery reaches its minimum state of charge, whereas aggregated approaches can conceal or artificially create those events. Prior research on PV-battery modeling has demonstrated that simulation time resolution can affect self-consumption and system sizing, although the magnitude of the effect depends on the system configuration and the variables being optimized [5]. Studies of high-frequency PV variability likewise show that temporal averaging removes information about ramps and peaks [6]. More recent work on hybrid CSP–PV systems confirms that coarser time steps can lose operational information even when annual energy remains similar [7].

The present study isolates a narrower and more fundamental question: how much reliability error is introduced solely by replacing a native hourly solar-resource sequence with daily-to-hourly reconstructions. Three temporal treatments are compared. H is the native hourly NASA POWER series. D_flat conserves each observed daily GHI total but distributes it uniformly over all 24 hourly intervals. D_sin also conserves the daily total, but redistributes it according to a daylight-weighted sinusoidal envelope derived from solar elevation. The two reconstructions therefore preserve daily energy by construction while making progressively stronger assumptions about intraday timing. The design makes it possible to distinguish errors caused by daily energy loss from errors caused by temporal shape.

The study has five objectives. First, it quantifies the effect of temporal treatment on simulated PV energy production across six climate-diverse sites. Second, it measures the effect on chronological LPSP and longest continuous outage under a common PV – battery configuration. Third, it determines the nominal battery capacity required to achieve 1% and 0.1% unmet-load-hour targets. Fourth, it evaluates whether the observed differences are statistically consistent across the six sites rather than being driven by a single climate. Fifth, it performs a one-factor sensitivity analysis for load, PV size, round-trip efficiency, maximum depth of discharge, and initial SOC.

The contribution is methodological and practical. The analysis does not propose a new PV cell model or a new battery electrochemistry model. Instead, it demonstrates that the temporal representation of the same underlying daily solar resource can materially alter reliability conclusions in chronological PV – battery simulations. This distinction is important for computational studies because a seemingly harmless daily averaging step can become a structural modeling assumption. The paper therefore treats temporal resolution as a model parameter that should be reported, justified, and subjected to sensitivity analysis rather than as a neutral data-processing choice.

RELATED WORK

Solar-resource conversion from horizontal to tilted planes is a mature but nontrivial problem. Solar position determines the incidence angle and the daylight envelope; Reda and Andreas provide a high-accuracy solar-position algorithm for radiation applications [8]. Diffuse radiation can be estimated from global horizontal irradiance using empirical clearness-index relationships [2]. For tilted surfaces, Perez-type models and the family of isotropic and anisotropic transposition models provide established alternatives [9], [10]. The present work intentionally uses a transparent isotropic transposition formulation rather than selecting a more

elaborate anisotropic model because the research question concerns relative differences between temporal treatments, and the same conversion model is applied to all treatments.

PV output is affected by irradiance, module temperature, optical losses, and electrical characteristics. Simplified PV output formulations have a long history [11], while the Sandia PV Array Performance Model explicitly incorporates irradiance, thermal, and optical effects for hourly simulations [12]. PVWatts provides a compact model in which nameplate power is scaled by effective irradiance and corrected using a temperature coefficient [13]. Module temperature can be represented with simple empirical heat-transfer formulations such as the Faiman model, which relates module temperature to ambient temperature, plane-of-array irradiance, and wind speed [14]. Reviews of PV temperature behavior emphasize that the power-temperature coefficient is material and module dependent, supporting the use of a transparent generic coefficient when a specific module datasheet is not available [15].

Solar-resource databases themselves are also an established research topic. Satellite-based databases such as PVGIS have demonstrated that hourly solar radiation estimates can support PV performance assessment over broad geographic regions [16]. The accuracy and representativeness of gridded or satellite-derived resource data vary spatially, so the present results should be interpreted as a comparative computational experiment rather than as a claim that the simulated PV output is equivalent to measured field production. The objective is to hold the resource source constant and alter only the temporal treatment.

Temporal resolution has received increasing attention in PV and energy-system studies. Li et al. showed that minutely PV simulation can capture transient characteristics that hourly modeling cannot reproduce, with daily energy differences depending on weather conditions [17]. Kreuwel et al. demonstrated that temporal averaging can suppress high-frequency PV fluctuations and peak values [6]. Zurita et al. found that coarse temporal resolution can lose variability information in hybrid CSP–PV modeling [7]. Beck et al. examined the influence of temporal resolution on PV-battery self-consumption and sizing and found that the relevant resolution depends on the system objective and load characteristics [5]. These studies motivate the present focus on reliability rather than only annual yield.

For stand-alone PV systems, reliability is commonly expressed through loss-of-power-supply probability or related loss-of-load indices. LPSP-based sizing methods are widely reviewed in the literature [18], and chronological sizing approaches explicitly simulate the battery SOC over time. Shen demonstrated the use of LPSP in PV and battery sizing [19], while Aziz et al. compared iterative and computational-intelligence sizing approaches using LPSP as a reliability criterion [20]. The reliability metric is sensitive to battery modeling assumptions; Ibrahim et al. showed that battery-model complexity can materially change sizing results [21]. Detailed battery models can represent rate, temperature, and electrochemical effects [22]–[24], with the newer models explicitly demonstrating the importance of partial-charge and thermal behavior [23]. A simplified energy-balance battery is widely used when the research question is system-level temporal behavior rather than battery degradation or voltage dynamics. This study follows that approach and treats charge and discharge efficiency symmetrically as the square root of the specified round-trip efficiency.

The literature on solar-power forecasting and variability likewise emphasizes that the temporal structure of the solar resource affects system interpretation and uncertainty [25]. The literature also indicates that SOC assumptions matter. Elshurafa and Aldubyan examined the effect of state-of-charge constraints in stand-alone PV-battery systems and showed that storage behavior can materially influence technical and economic outcomes [26]. Consequently, the present study reports its initial SOC assumption explicitly and tests a lower initial SOC in sensitivity analysis.

Finally, the interpretation of temporal-treatment differences requires statistical care. Because the same six sites are evaluated under all three treatments, the primary comparison is paired rather than independent. Friedman's nonparametric repeated-measures test is appropriate for a small number of sites without assuming normality [27], and pairwise Wilcoxon signed-rank tests can identify the direction of treatment differences [28]. Holm's step-down procedure is used to control family-wise error across pairwise comparisons [29]. Confidence intervals are obtained with year-block bootstrap resampling, following the general resampling framework introduced by Efron [30]. This statistical design is intentionally conservative: the six sites are the experimental units, while the hourly observations are the chronological inputs used to generate the site-level outcomes.

MATERIALS AND METHODS

Study Design and Locations

The empirical dataset comprises six single-point NASA POWER hourly files covering 1 January 2019 through 31 December 2023 in UTC. The six locations were selected to span strong contrasts in solar resource and seasonality: Phoenix and Tucson represent hot-arid conditions; Atlanta represents humid subtropical conditions; London represents an oceanic climate; Munich represents temperate central-European conditions; and Rovaniemi represents a subarctic high-latitude environment. The geographic coordinates were taken directly from the POWER file headers. All six files contain 43,824 hourly records, corresponding to the five-year period including leap day in 2020, and none of the three required variables contains a missing-value code. Figure 1 maps the geographic distribution of the six study locations.

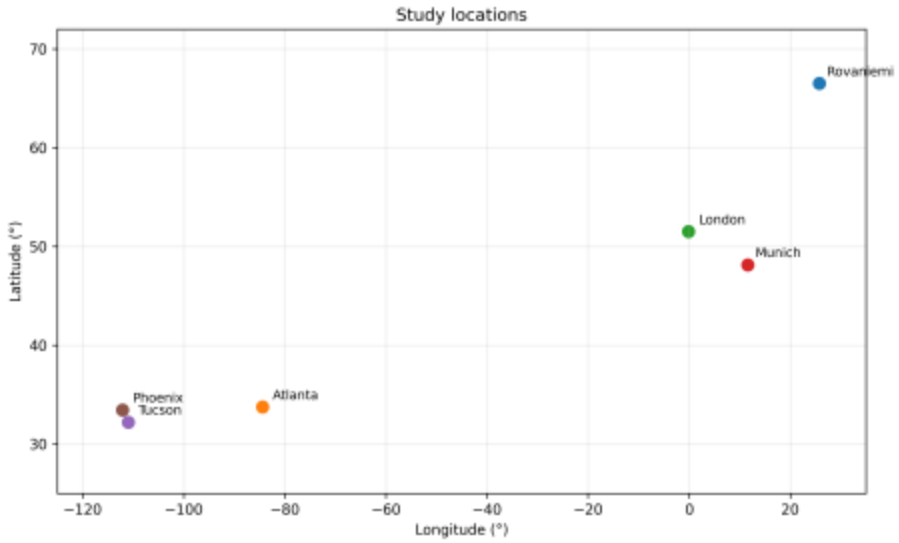


Figure 1. Geographic distribution of the six study locations

The NASA POWER variables are ALLSKY_SFC_SW_DWN, T2M, and WS10M [4]. ALLSKY_SFC_SW_DWN is hourly surface shortwave downward irradiation in Wh m^2, while T2M is air temperature at 2 m and WS10M is wind speed at 10 m. The hourly irradiation values are numerically equivalent to hourly mean irradiance in W m^2 because the interval is one hour. The analysis uses the files supplied for this study without gap filling or stochastic replacement. This is important because artificial interpolation could itself alter the temporal-variability question being studied.

Solar-day Alignment

Although the downloaded data are in UTC, daily reconstruction is performed on a local-mean-solar basis. For each site, UTC time is shifted by longitude/15 hours to obtain local mean solar time. A solar day is then defined by the resulting calendar date. This avoids using civil-time boundaries that are unrelated to the sun and ensures that the daily GHI total used in D_flat and D_sin corresponds to one solar-day interval.

Temporal Treatments

Three treatments are compared.

H (native hourly): the original hourly GHI sequence is retained.

Dflat (24-h flat reconstruction): the observed daily *GHI* total *Hd* is divided equally among all 24 hourly intervals:

$$G_{flat}(t) = \frac{H_d}{24} \quad (1)$$

This is deliberately a strong smoothing assumption. It preserves daily energy but does not preserve daylight timing. Consequently, the treatment tests the extreme case in which a daily energy total is converted to hourly data without solar-geometry information.

Dsin (daylight sinusoidal reconstruction): the same daily total is distributed only over daylight hours using the positive part of solar elevation:

$$G_{sin}(t) = \frac{H_d w_t}{\sum_{j \in d} w_j}, \text{ where } w_t = \max[\sin(\alpha_t), 0] \quad (2)$$

where αt is solar elevation at the midpoint of hour t. Equation (2) conserves the observed daily GHI exactly while imposing a physically interpretable daylight envelope. The procedure is intentionally simple; it is not intended to reproduce cloud transients within a day.

Solar Geometry and Plane-of-Array Irradiance

Solar zenith and azimuth are calculated from standard astronomical solar-position equations consistent with established solar-radiation practice [8]. The reference PV array is fixed at a tilt equal to the absolute site latitude and faces due south because all six sites are in the Northern Hemisphere. No shading or horizon obstruction is assumed.

Because only GHI is supplied, diffuse horizontal irradiance is estimated using the Erbs clearness-index relationship [2]. The hourly clearness index is

$$k_t = \frac{GHI}{G_{0,h}} \quad (3)$$

where G_0, h is extraterrestrial horizontal irradiation for the hour. Diffuse fraction is then obtained from the piecewise Erbs correlation, and direct normal irradiance is derived from the direct horizontal component divided by the cosine of solar zenith angle when the sun is above the horizon.

For the reference plane, an isotropic diffuse transposition is used:

$$G_{POA} = DNI \cdot \max[\cos(\theta_i), 0] + DHI\frac{1+\cos(\beta)}{2} + \rho_g GHI\frac{1-\cos(\beta)}{2} \quad (4)$$

where θi is the incidence angle, β is the fixed tilt, and $\rho g=0.20$ is the assumed ground albedo. The isotropic formulation is transparent and reproducible, although the literature shows that anisotropic models can provide better tilted-plane performance in some conditions [10]. A direct-beam incidence-angle modifier is applied using the ASHRAE form with b=0.05; diffuse IAM is held at unity. The same assumptions are used for all temporal treatments, so they cannot explain differences between H, D_{flat}, and Dsin.

PV Power Model

The reference PV array has a nominal rating of 10 Wp. A generic PVWatts-type model is used [13]. Effective irradiance is the direct POA component after the incidence-angle modifier plus the diffuse and ground-reflected components. Module temperature follows the Faiman relationship [14]:

$$T_m = T_a + \frac{G_{POA}}{U_0 + U_1 WS} \quad (5)$$

with U_0=25 W m^2 K−1 and U_1=6.84 W m^3 s K−1. The DC power is then calculated as

$$P_{DC} = P_0 \left(\frac{G_{eff}}{1000}\right)[1 + \gamma(T_m - 25)] \quad (6)$$

The DC-bus PV power used in the energy-balance simulation was calculated by applying a fixed DC-path efficiency of 95% to the modeled DC output, i.e., $P_{PV,\ t=0.95}\ P_{DC,\ t}$. The generic coefficient is consistent with the linear temperature dependence commonly used in simplified PV models [15], while the use of a nominal rather than manufacturer-specific module reflects the system-level focus of the study.

Load and Battery Model

The baseline load is a constant 2 W DC demand, giving 17.52 kWh yr−1. The reference battery has 50 Wh nominal capacity, 12-V nominal voltage, 80% maximum depth of discharge (DoD), and 85% round-trip efficiency. The usable energy is therefore 0.8C, where C is nominal capacity. Charge and discharge efficiencies are each set to √0.85. The initial SOC is 100% of usable capacity.

The hourly energy-balance rule is chronological. When PV exceeds the load, the surplus charges the battery until the usable upper limit is reached. When PV is below the load, the deficit is supplied from the battery subject to the minimum SOC. If the battery cannot supply the full deficit, the remaining load is classified as unmet. This simplified energy-balance formulation is widely used for system-level PV-battery studies, although detailed battery models can alter the numerical result [21]–[24]. The purpose here is to isolate temporal-resource effects rather than electrochemical behavior.

Reliability Metrics

The primary reliability metric is the fraction of hourly load intervals with any unmet demand

$$LPSP_h = \frac{N_{fail}}{N} \quad (7)$$

where N_{fail} is the number of hours in which the battery is unable to satisfy the full 2-W load and N=43,824. A secondary energy-deficit fraction is also calculated:

$$LPSP_E = \frac{\sum E_{unmet}}{\sum E_{load}} \quad (8)$$

Where E_{unmet} , t represents the unmet load energy during hour t, and E_{load}, t represents the total demanded load energy during hour t.

The longest continuous outage is calculated as the maximum consecutive run of failure hours. Reporting both time-based and energy-based indices avoids overinterpreting a single reliability metric, since LPSP variants can emphasize different aspects of shortage behavior [18].

Battery Sizing

For each site and temporal treatment, nominal battery capacity is increased monotonically until the target LPSP_h is reached. Two targets are used: 1% and 0.1%. A binary search is applied between 1 Wh and 5,000 Wh. If the target is not reached at 5,000 Wh, the case is reported as infeasible rather than extrapolated. Battery capacity is also converted to Ah at 12 V for interpretability.

The initial SOC is deliberately held at 100% for the primary sizing experiment. This makes the reported capacity a five-year conditional sizing result: the system is assumed to enter the study period with a fully charged battery. The study does not claim a cyclic or lifetime-optimal battery size, because enforcing equal initial and terminal SOC would require an energy-neutrality condition that several sites do not satisfy under the reference 10-Wp PV and 2-W load.

Sensitivity Analysis

One-factor-at-a-time sensitivity analysis is performed at the native-hourly 99% battery capacity for the two sites for which the baseline system is energy-feasible. The tested changes are load of 1 W and 3 W, PV rating of 5 Wp and 20 Wp, round-trip efficiency of 80% and 90%, maximum DoD of 70% and 90%, and initial

SOC of 80%. The baseline case remains 2 W, 10 Wp, 85%, 80% DoD, and 100% initial SOC. This design identifies which assumptions most strongly alter LPSP without introducing the additional confounding of simultaneous parameter changes.

Statistical Analysis

The six sites are treated as paired experimental units. The primary omnibus test is the Friedman test across *H, Dflat*, and *Dsin*. Kendall's W is reported as an effect-size measure. Pairwise Wilcoxon signed-rank tests compare *H* with *Dflat*, *H* with *Dsin*, and *Dsin* with *Dflat*, with Holm adjustment for three comparisons [27]–[29]. Statistical significance is assessed at α=0.05.

To provide uncertainty intervals without assuming independent hourly observations, a year-block bootstrap is used. The five annual LPSP values at each site are resampled with replacement 20,000 times, and the 2.5th and 97.5th percentiles form the 95% interval [30]. These intervals quantify variability across the observed five-year blocks; they do not represent uncertainty in the NASA POWER product, PV model, battery model, or climate projection.

All analysis was implemented in Python using deterministic numerical routines. The input files were checked for record completeness, missing-value codes, and daily-energy conservation after temporal reconstruction.

RESULTS

Data Completeness and Climate Contrast

All six uploaded POWER files contain the full 43,824 hourly records required for 2019−2023, with no missing values in GHI, T2M, or WS10M. Table 1 summarizes the site characteristics and resource-variability indicators. The annual mean GHI spans a factor of approximately 2.55 between Rovaniemi and Phoenix. Phoenix has the highest mean annual GHI at 2,133.4 kWh m−2 yr−1, closely followed by Tucson at 2,119.7 kWh m^2 yr−1. Atlanta records 1,657.2 kWh m^2 yr−1, Munich 1,231.4 kWh m^2 yr−1, London 1,110.2 kWh m^2 yr−1, and Rovaniemi 838.4 kWh m^2 yr−1. The resource ranking is therefore strongly climate dependent.

Table 1. Study Sites, Climate Settings, and Solar-Resource Variability

Site	Latitude	Longitude	Climate setting	Annual GHI (kWh m^{-2} yr^{-1})	Daily GHI CV	Monthly GHI CV	Daylight-hour GHI CV
Rovaniemi	66.5039	25.7294	Subarctic	838.364	0.973	0.891	0.919
Atlanta	33.7490	-84.3880	Humid subtropical	1657.187	0.442	0.323	0.715
London	51.5072	-0.1276	Oceanic	1110.169	0.681	0.590	0.819
Munich	48.1372	11.5756	Temperate continental	1231.442	0.654	0.559	0.815
Tucson	32.2226	-110.9747	Hot desert	2119.732	0.337	0.299	0.622
Phoenix	33.4484	-112.0740	Hot desert	2133.352	0.342	0.316	0.618

Daily GHI variability is also strongly differentiated. The coefficient of variation of daily GHI is 0.337 in Tucson and 0.342 in Phoenix, compared with 0.442 in Atlanta, 0.654 in Munich, 0.681 in London, and 0.973 in Rovaniemi. The high-latitude site consequently combines a lower resource with greater day-to-day variability. Monthly variability follows a similar pattern, with monthly GHI CV values of approximately 0.30 – 0.32 in the two desert sites, 0.56 – 0.59 in Munich and London, and 0.92 in Rovaniemi. These differences provide an appropriate test bed for examining whether a temporal reconstruction behaves similarly across climates.

Effect of Temporal Reconstruction on PV Energy

Figure 2 shows the daily-GHI distributions, and Figure 3 illustrates the contrasting temporal profiles. The native hourly treatment produces 10-Wp annual PV energies of 20.17 kWh in Phoenix, 20.24 kWh in Tucson,

15.92 kWh in Atlanta, 11.97 kWh in Munich, 10.97 kWh in London, and 8.55 kWh in Rovaniemi. The annual energy ranking therefore mirrors the underlying solar resource.

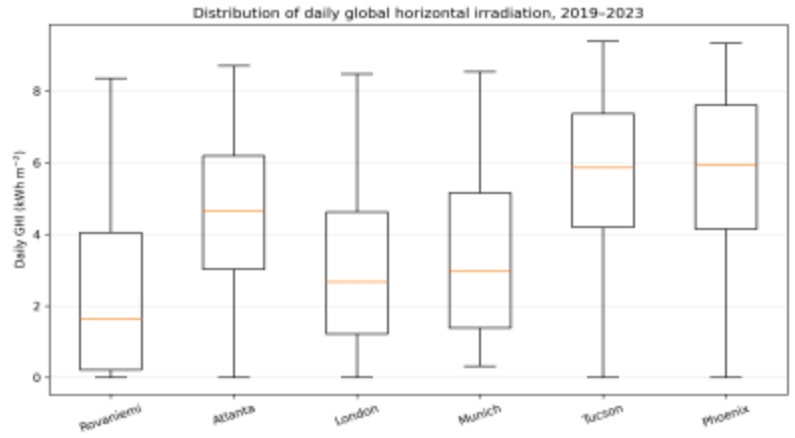


Figure 2. Distribution of Daily Global Horizontal Irradiation During 2019–2023

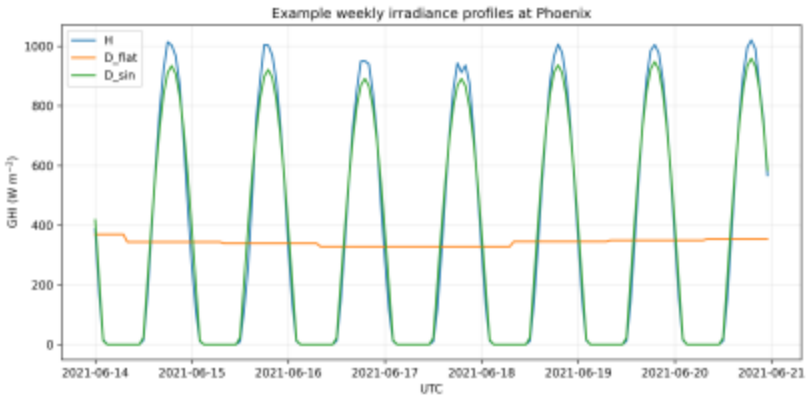


Figure 3. Example One-Week GHI Profiles at Phoenix Under the Native Hourly, Flat Daily, and Sinusoidal Daily Treatments

D_flat systematically reduces simulated PV energy. Relative to H, the annual reduction is 13.3% in Phoenix, 12.4% in Tucson, 12.1% in Atlanta, 19.8% in Munich, 22.8% in London, and 38.8% in Rovaniemi. The effect is not a numerical artifact of changing daily energy totals: the daily GHI total is conserved exactly before the PV conversion. Rather, the flat profile assigns part of the daily energy to hours with unfavorable solar geometry, including nighttime intervals. This converts a daily-average assumption into an intraday generation assumption and thereby changes the plane-of-array irradiance seen by the PV model.

D_sin is substantially closer to H. Annual PV energy differs from H by −0.8% in Phoenix, −0.7% in Tucson, −1.0% in Atlanta, −2.8% in Munich, −3.2% in London, and −5.7% in Rovaniemi. The residual difference increases at high latitude because the daylight envelope becomes more seasonally asymmetric and because the sinusoidal reconstruction does not reproduce within-day cloud structure. Nevertheless, D_sin preserves the annual energy scale much more faithfully than D_flat.

The Friedman test for annual PV energy gives χ^2=12.00, p=0.0025, with Kendall's W=1.00. Thus, across all six sites, the temporal treatments produce a consistent ranking: H has the highest annual PV yield, D_sin is close behind, and D_flat is lowest.

Baseline LPSP and Outage Duration

Table 2 reports the complete baseline numerical results. The 50-Wh baseline battery does not provide high reliability at all sites. Under H, LPSP_h is 6.41% in Phoenix and 6.70% in Tucson. Atlanta has 24.06%,

Munich 44.82%, London 50.04%, and Rovaniemi 62.09%. The longest continuous outage is 44 h in Phoenix, 58 h in Tucson, 83 h in Atlanta, 283 h in Munich, 593 h in London, and 2,278 h in Rovaniemi. These values show that the same PV and battery hardware can move from marginal reliability to extreme unreliability solely because of climate.

Table 2. Baseline PV Energy and Reliability Results for the 50-Wh Battery

Site	Scenario	Annual PV energy (kWh/yr)	LPSP (%)	Unmet energy (%)	Longest outage (h)
Rovaniemi	H	8.55	62.09	55.21	2278
Rovaniemi	D_flat	5.23	96.39	70.17	5933
Rovaniemi	D_sin	8.06	64.71	56.91	2301
Atlanta	H	15.92	24.06	19.62	83
Atlanta	D_flat	14.00	48.90	22.04	361
Atlanta	D_sin	15.75	24.59	19.88	126
London	H	10.97	50.04	42.56	593
London	D_flat	8.47	88.36	51.88	3031
London	D_sin	10.62	51.88	43.65	613
Munich	H	11.97	44.82	37.89	283
Munich	D_flat	9.59	79.58	45.64	2535
Munich	D_sin	11.63	46.55	38.81	404
Tucson	H	20.24	6.70	5.56	58
Tucson	D_flat	17.74	26.78	9.11	136
Tucson	D_sin	20.10	6.52	5.48	56
Phoenix	H	20.17	6.41	5.30	44
Phoenix	D_flat	17.47	28.81	9.82	231
Phoenix	D_sin	20.00	6.08	5.08	59

Figure 4 summarizes the cross-site LPSP comparison. D_flat produces a much larger reliability penalty. LPSP rises to 28.81% in Phoenix and 26.78% in Tucson, 48.90% in Atlanta, 79.58% in Munich, 88.36% in London, and 96.39% in Rovaniemi. Relative to H, these are increases of 349.4%, 299.8%, 103.3%, 77.6%, 76.6%, and 55.3%, respectively. The ordering is striking: the largest relative error occurs in the two best solar climates because their native hourly systems are close to the threshold at which short-term timing determines whether the battery is depleted. Smoothing the resource destroys this favorable timing.

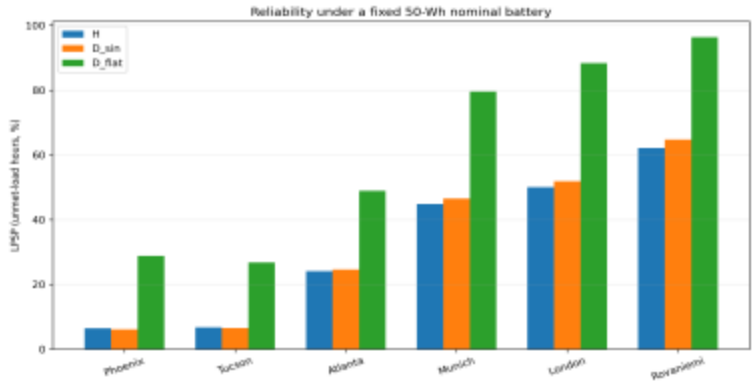


Figure 4. LPSP Under the Common 50-Wh Nominal Battery across the Six Sites

D_sin performs much better. LPSP is 6.08% in Phoenix, 6.52% in Tucson, 24.59% in Atlanta, 46.55% in Munich, 51.88% in London, and 64.71% in Rovaniemi. Relative to H, the changes range from −5.1% in Phoenix to +4.2% in Rovaniemi. The longest outage is also much closer to the native-hourly value than under D_flat.

Table 3 summarizes the inferential tests, while Table 4 gives the year-block bootstrap intervals. The primary Friedman test confirms that the three temporal treatments differ in LPSP across the six sites (χ^2=9.33,

p=0.0094, Kendall's W=0.78). Pairwise Wilcoxon tests give unadjusted p=0.031 for H versus D_flat, p=0.156 for H versus D_sin, and p=0.031 for D_sin versus D_flat. After Holm adjustment, none of the individual pairwise comparisons remains below 0.05, which is expected given the small number of paired sites. The appropriate interpretation is therefore that the omnibus evidence for a treatment effect is strong, while the study has limited power for corrected pairwise inference.

Table 3. Statistical Comparison of Temporal Treatments

Test	Statistic	Unadjusted p	Effect / adjusted p
Friedman: LPSP	9.333	0.0094	Kendall W=0.7778
Wilcoxon: H vs D_flat	0.000	0.0312	Holm p=0.0938
Wilcoxon: H vs D_sin	3.000	0.1562	Holm p=0.1562
Wilcoxon: D_sin vs D_flat	0.000	0.0312	Holm p=0.0938
Friedman: annual PV energy	12.000	0.0025	Kendall W=1.0000

Table 4. Year-Block Bootstrap 95% Confidence Intervals for Baseline LPSP

Site	H: LPSP % [95% CI]	D_sin: LPSP % [95% CI]	D_flat: LPSP % [95% CI]
Atlanta	24.05% [22.38, 24.05]	24.59% [22.88, 24.60]	48.90% [45.75, 48.90]
London	50.04% [47.93, 50.04]	51.88% [49.80, 51.88]	88.37% [86.14, 88.37]
Munich	44.82% [43.52, 44.82]	46.55% [45.08, 46.55]	79.58% [77.16, 79.58]
Phoenix	6.41% [5.10, 6.41]	6.08% [4.77, 6.08]	28.81% [27.32, 28.81]
Rovaniemi	62.09% [61.10, 62.09]	64.71% [63.56, 64.71]	96.39% [95.82, 96.39]
Tucson	6.70% [5.48, 6.70]	6.52% [5.33, 6.52]	26.78% [26.09, 26.78]

Energy-Based Shortage Metric

The energy-based deficit fraction follows the same pattern but is less extreme than the hour-based LPSP in some cases. Under H, the unmet-energy fraction is 5.30% in Phoenix, 5.56% in Tucson, 19.62% in Atlanta, 37.89% in Munich, 42.56% in London, and 55.21% in Rovaniemi. D_flat increases these values to 9.82%, 9.11%, 22.04%, 45.64%, 51.88%, and 70.17%, respectively. D_sin remains close to H, at 5.08%, 5.48%, 19.88%, 38.81%, 43.65%, and 56.91%.

The agreement between the two LPSP formulations is important. The temporal-resolution effect is not merely a consequence of counting a small number of low-energy outage hours. D_flat changes both the frequency and the magnitude of energy deficits. The effect is especially large at Phoenix and Tucson because the native hourly sequence contains substantial daytime surplus that can be stored and used across short cloudy intervals, whereas the flat reconstruction disrupts the timing of that surplus.

Battery Capacity Required for 1% and 0.1% LPSP

At the reference 10-Wp PV and 2-W load, the 1% and 0.1% LPSP targets are not reached within the 5,000-Wh search limit for Rovaniemi, London, Munich, or Atlanta under any temporal treatment. This is not simply a battery-sizing problem. The five-year PV energy produced by the reference array is below the total load energy at those sites. For example, native-hourly PV supplies only about 91% of annual load energy in Atlanta, 68% in Munich, 63% in London, and 49% in Rovaniemi. No finite battery can compensate indefinitely for a persistent source-energy deficit.

The two desert sites are different. Table 5 gives the corresponding battery-sizing results, and Figure 5 visualizes the feasible cases. Under H, the nominal battery required for 1% LPSP is 727 Wh in Phoenix and 640 Wh in Tucson. For the stricter 0.1% target, the requirements increase to 1,071 Wh and 1,025 Wh, respectively. D_sin produces slightly smaller requirements: 620 Wh and 592 Wh for the 1% target, and 971 Wh and 953 Wh for the 0.1% target. D_flat produces dramatically larger requirements: 3.82 kWh in Phoenix and 2.45 kWh in Tucson for 1% LPSP, increasing to 4.12 and 2.78 kWh for 0.1% LPSP.

Table 5. Nominal Battery Capacity Required to Meet the Specified LPSP Targets

Site	Scenario	Target LPSP (%)	Nominal battery (Wh)	Nominal battery (Ah at 12 V)	Usable energy (Wh)
Rovaniemi	H	1.0	Infeasible	Infeasible	Infeasible
Rovaniemi	H	0.1	Infeasible	Infeasible	Infeasible
Rovaniemi	D_flat	1.0	Infeasible	Infeasible	Infeasible
Rovaniemi	D_flat	0.1	Infeasible	Infeasible	Infeasible
Rovaniemi	D_sin	1.0	Infeasible	Infeasible	Infeasible
Rovaniemi	D_sin	0.1	Infeasible	Infeasible	Infeasible
Atlanta	H	1.0	Infeasible	Infeasible	Infeasible
Atlanta	H	0.1	Infeasible	Infeasible	Infeasible
Atlanta	D_flat	1.0	Infeasible	Infeasible	Infeasible
Atlanta	D_flat	0.1	Infeasible	Infeasible	Infeasible
Atlanta	D_sin	1.0	Infeasible	Infeasible	Infeasible
Atlanta	D_sin	0.1	Infeasible	Infeasible	Infeasible
London	H	1.0	Infeasible	Infeasible	Infeasible
London	H	0.1	Infeasible	Infeasible	Infeasible
London	D_flat	1.0	Infeasible	Infeasible	Infeasible
London	D_flat	0.1	Infeasible	Infeasible	Infeasible
London	D_sin	1.0	Infeasible	Infeasible	Infeasible
London	D_sin	0.1	Infeasible	Infeasible	Infeasible
Munich	H	1.0	Infeasible	Infeasible	Infeasible
Munich	H	0.1	Infeasible	Infeasible	Infeasible
Munich	D_flat	1.0	Infeasible	Infeasible	Infeasible
Munich	D_flat	0.1	Infeasible	Infeasible	Infeasible
Munich	D_sin	1.0	Infeasible	Infeasible	Infeasible
Munich	D_sin	0.1	Infeasible	Infeasible	Infeasible
Tucson	H	1.0	640	53.3	512
Tucson	H	0.1	1025	85.5	820
Tucson	D_flat	1.0	2452	204.3	1962
Tucson	D_flat	0.1	2779	231.5	2223
Tucson	D_sin	1.0	592	49.3	474
Tucson	D_sin	0.1	953	79.4	762
Phoenix	H	1.0	727	60.6	582
Phoenix	H	0.1	1071	89.2	856
Phoenix	D_flat	1.0	3819	318.2	3055
Phoenix	D_flat	0.1	4117	343.1	3293
Phoenix	D_sin	1.0	620	51.7	496
Phoenix	D_sin	0.1	971	80.9	777

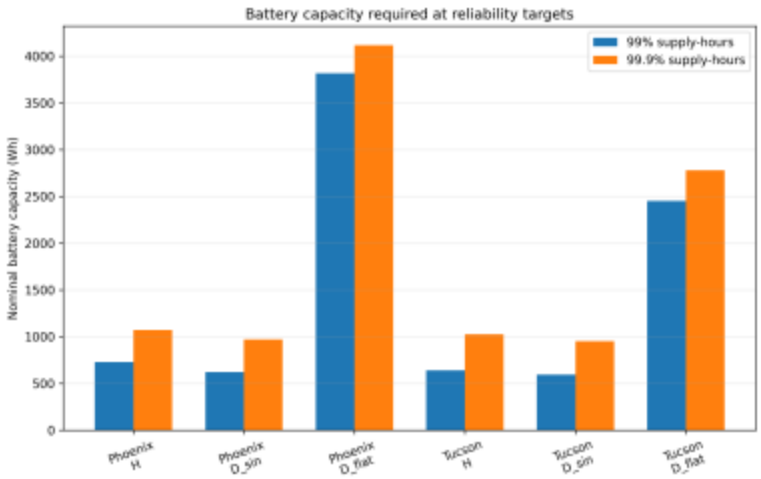


Figure 5. Nominal Battery Capacity Required for 1% and 0.1% LPSP in the Two Energy-Feasible Desert Sites

Thus, in the feasible desert cases, D_flat overstates the 1% battery requirement by 425% in Phoenix and 283% in Tucson. D_sin instead reduces the requirement by 14.8% and 7.4%, respectively, relative to H. The difference is operationally important because the battery capacities are no longer a small perturbation around

a common design value; the choice of temporal reconstruction can move the design from a sub-kWh storage system to several kilowatt-hours.

The 12-V equivalents are 60.6 Ah for the Phoenix H 1% case and 53.3 Ah for Tucson. The corresponding 0.1% capacities are 89.2 Ah and 85.5 Ah. These figures should not be interpreted as manufacturer-specific battery recommendations because the model uses a generic energy-balance battery, a fixed 12-V nominal voltage, and an initial full charge.

Sensitivity Analysis

Table 6 and Figure 6 summarize the sensitivity results. The sensitivity analysis confirms that the temporal treatment interacts with system sizing but is not the only determinant of reliability. At the H-derived 99% battery capacity, reducing the load from 2 W to 1 W eliminates modeled outages in both Phoenix and Tucson. Increasing the load to 3 W raises LPSP to 34.13% in Phoenix and 33.88% in Tucson. Reducing PV from 10 to 5 Wp produces an even stronger deterioration, with LPSP of 51.76% in Phoenix and 51.32% in Tucson. Increasing PV to 20 Wp eliminates modeled outages in both sites.

Table 6. One-Factor Sensitivity of LPSP at the Native-Hourly 99% Battery Capacity

Scenario	Phoenix LPSP (%)	Tucson LPSP (%)
baseline	1.00	1.00
load_1W	0.00	0.00
load_3W	34.13	33.88
pv_5Wp	51.76	51.32
pv_20Wp	0.00	0.00
eta_rt_0.80	2.29	2.24
eta_rt_0.90	0.34	0.55
DoD_0.70	1.38	1.31
DoD_0.90	0.65	0.72
initial_soc_0.80	1.00	1.13

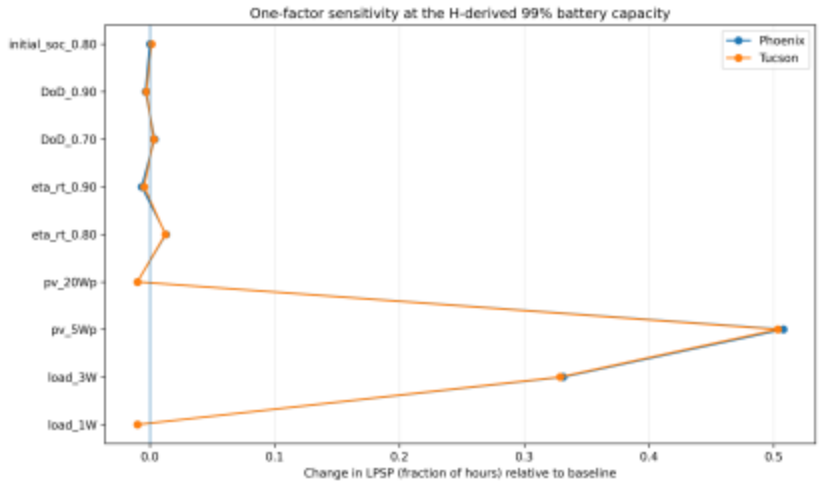


Figure 6. One-Factor Sensitivity of LPSP Relative to the Native-Hourly Baseline at the 99% Battery Capacity

Battery efficiency has a meaningful but smaller effect. Reducing round-trip efficiency from 85% to 80% raises Phoenix LPSP from 1.00% to 2.29% and Tucson LPSP from 1.00% to 2.24%. Increasing efficiency to 90% reduces LPSP to 0.34% and 0.55%, respectively. Maximum DoD also matters: reducing DoD from 80% to 70% increases LPSP to 1.38% in Phoenix and 1.31% in Tucson, while increasing DoD to 90% reduces LPSP to 0.65% and 0.72%.

The 80% initial-SOC scenario has only a small effect over the five-year horizon: LPSP becomes 1.00% in Phoenix and 1.13% in Tucson. This is because the initial reserve is quickly absorbed into the chronological

energy balance and has limited influence on the long-run sequence. Nevertheless, the result reinforces the importance of reporting the initial SOC rather than treating it as an implicit modeling detail.

DISCUSSION

The central finding is that daily energy conservation does not guarantee reliability conservation. D_flat preserves every observed daily GHI total exactly, yet it produces substantially different PV energy and much worse battery reliability. The reason is chronological: a battery stores energy when it is available and supplies energy when it is not. The order of those events is part of the system state. A temporal transformation that changes the order, even while preserving the daily integral, changes SOC trajectories.

The magnitude of the D_flat bias is particularly revealing. The bias is largest in the two desert locations, where the native hourly system is comparatively energy rich. It might be expected that a strong solar resource would make the system less sensitive to temporal resolution. The opposite occurs in relative terms. When the system is close to a reliability threshold, the timing of a few long deficit sequences can dominate the LPSP. A flat reconstruction removes the daytime concentration of PV and therefore removes the ability to recharge the battery during the hours in which the PV array actually operates most effectively. The resulting reliability penalty is not a simple function of annual solar resource.

D_sin provides a useful intermediate result. It uses exactly the same daily GHI totals as D_flat but imposes a solar-geometry-informed daylight envelope. Its annual PV energy is within 0.8−5.7% of H, and its LPSP differs from H by only −5.1% to +4.2%. This suggests that when only daily solar data are available, a physically constrained daylight reconstruction is preferable to a uniform 24-h allocation. The result is consistent with the broader solar-resource literature, which treats solar position and the diurnal radiation structure as fundamental inputs to irradiance modeling [1]–[2], [8]–[10].

However, D_sin is not equivalent to H. The remaining difference is attributable to cloud timing and other intraday weather structure that cannot be reconstructed from daily totals alone. At Rovaniemi, for example, the daily-to-sinusoidal reconstruction raises LPSP from 62.09% to 64.71%, a modest but systematic difference in a climate with very strong seasonal and daily variation. The D_sin method therefore should be understood as a structured approximation, not as a substitute for measured or high-quality hourly resource data.

The results also illustrate why PV-battery reliability should not be evaluated using annual energy balance alone. Atlanta has a native-hourly annual PV yield of 15.92 kWh for the 10-Wp array against approximately 17.52 kWh of annual load. This immediately indicates that the baseline system cannot achieve very high reliability over a multi-year continuous simulation. But Phoenix and Tucson have annual PV production exceeding annual load, yet the 50-Wh battery still produces approximately 6.4−6.7% LPSP. This occurs because energy surplus and energy deficit are not perfectly synchronized. The battery must bridge nights, cloudy intervals, and seasonal deficits. LPSP therefore captures a dimension of adequacy that annual energy ratios cannot.

The battery-sizing results provide a practical consequence. Under the native hourly treatment, the desert sites require approximately 0.6−0.7 kWh nominal storage for 1% unmet-load hours and about 1.0−1.1 kWh for 0.1%. The D_flat reconstruction increases those requirements by several hundred percent. A designer who used D_flat without recognizing its temporal assumption could therefore oversize the battery by multiple kilowatt-hours. Conversely, using an overly smooth representation could distort comparisons between sites and lead to incorrect conclusions about which climate is most favorable.

These findings complement earlier work showing that temporal resolution affects PV-battery modeling, but they add a different perspective. Beck et al. found that hourly resolution can be adequate for some PV-battery sizing objectives when the input profiles are realistic [5]. The present experiment shows that the important distinction is not simply “hourly versus daily” but “native chronology versus reconstructed chronology.” An hourly profile generated from a daily total is still an hourly dataset, but it does not contain the same temporal information as an observed hourly series. The practical implication is that model documentation should report not only the nominal time step but also how each time step was constructed.

The study also highlights the interaction between temporal resolution and model complexity. Detailed battery electrochemical models can improve physical realism [21]–[24], but a more complex battery model

cannot recover temporal information that was removed from the solar input. If the irradiance chronology is incorrect, increasing battery-model sophistication does not solve the primary information deficit. The order of model priorities should therefore be: preserve the resource chronology where possible, document the temporal reconstruction when necessary, and then select battery complexity appropriate to the research question.

The climate comparison reinforces the importance of site diversity. The six sites show a continuum from energy-rich, relatively stable desert conditions to high-latitude, strongly seasonal conditions. Rovaniemi has nearly three times the daily GHI coefficient of variation of Tucson and a much lower annual solar resource. The same 10-Wp/50-Wh system therefore exhibits radically different reliability. A study based on one location could easily misrepresent the magnitude or even the direction of temporal-resolution effects.

The statistical analysis should be interpreted with the sample size in mind. The Friedman test is significant for both LPSP and annual PV energy, and Kendall's W indicates a strong treatment effect. Yet only six sites are available, so the pairwise Wilcoxon tests have low power after Holm correction. The study therefore supports a robust descriptive conclusion and an omnibus statistical conclusion rather than broad universal claims. The results demonstrate that the effect exists across the selected sites, but they do not establish a universal effect size for every climate or PV configuration.

The bootstrap intervals also require careful interpretation. The intervals resample five annual blocks, so they describe how the site-level metric changes across alternative combinations of the observed years. They are not predictive intervals for future climates and do not account for uncertainty in NASA POWER irradiance estimates. The year-block approach is nevertheless preferable to treating 43,824 hourly observations as independent because the latter would produce artificially narrow intervals.

Several limitations should be acknowledged. First, the PV model is generic. The analysis does not use a specific module, inverter, or battery manufacturer. Second, the isotropic tilted-plane model is deliberately simple; anisotropic transposition models may change absolute PV output. Third, no shading, soiling, degradation, inverter clipping, battery aging, or temperature-dependent battery capacity is represented. Fourth, the load is a constant 2-W DC demand rather than a measured household or device profile. This choice isolates the weather-chronology effect but limits direct interpretation for real consumer systems. Fifth, the initial SOC is 100%, so the battery-sizing values are conditional on a full initial reserve. Sixth, the D_flat reconstruction is intentionally extreme and should not be confused with a recommended engineering method.

A further limitation concerns data provenance. NASA POWER provides spatially consistent satellite and model-derived resource information, but a POWER grid point is not a physical pyranometer at the city center. The analysis therefore measures the sensitivity of a model driven by POWER data rather than the sensitivity of an installed PV plant to a particular weather station. This is appropriate for the research question but should be stated clearly in any application of the results.

Despite these limitations, the study has a useful methodological implication for computational renewable-energy research. Temporal preprocessing is often treated as a technical step before the "real" simulation. The results show that it is part of the model itself. If daily solar data are converted to hourly values, the reconstruction rule should be reported alongside the PV and battery equations. If reliability is the endpoint, preserving the chronology of surplus and deficit periods is more important than preserving only daily or annual energy totals.

The findings also suggest a practical hierarchy for data selection. When a stand-alone PV-battery system is being evaluated, native hourly resource data should be preferred whenever available. If only daily data are available, a solar-geometry-informed reconstruction such as D_sin is preferable to a uniform 24-h distribution. If the system is highly storage constrained, reliability results should be tested under more than one temporal reconstruction because the storage requirement can be sensitive to intraday timing. For early-stage screening, D_sin may be a useful compromise, but final design should use measured or high-quality hourly data whenever possible.

The contribution should therefore be interpreted as a reproducible computational demonstration rather than a universal battery-sizing prescription. The numerical values are tied to the six sites, 2019–2023 weather sequence, 10-Wp PV reference, 2-W load, 50-Wh baseline battery, and stated model assumptions. What is more general is the direction of the methodological lesson: preserving the daily integral is not sufficient when the performance metric depends on chronological storage dynamics.

CONCLUSION

This five-year multi-climate simulation demonstrates that temporal treatment of solar-resource data can materially change the conclusions of PV-battery reliability studies. Using the same daily GHI totals, a 24-h flat reconstruction produced much lower PV energy and substantially higher LPSP than the native hourly sequence. Across the six sites, D_flat increased LPSP by 55−349% relative to H under the 50-Wh reference battery, while D_sin remained within approximately ±5% of H.

The battery-sizing results were even more consequential. For the two energy-feasible desert sites, the 1% LPSP requirement was approximately 0.59–0.73 kWh under H/D_sin but 2.45–3.82 kWh under D_flat. Four sites were not capable of meeting the reliability targets within the 5,000-Wh search range because the reference 10-Wp array did not provide enough total energy relative to the continuous 2-W load. The analysis therefore separates two fundamentally different constraints: insufficient total energy cannot be solved by storage, while poor temporal alignment can be mitigated by storage.

The statistical results support the overall conclusion. Friedman's test identified a significant effect of temporal treatment on both LPSP and annual PV energy, with strong site-paired effect sizes. The corrected pairwise tests were less powerful because only six sites were available, so the statistical evidence should be described as an omnibus demonstration rather than a universal pairwise claim.

The main engineering recommendation is straightforward: native hourly resource data should be used whenever reliability or battery sizing is the objective. If only daily resource totals are available, a daylight- and solar-geometry-informed reconstruction is preferable to uniform 24-h allocation, but it should be treated as an approximation. Most importantly, temporal reconstruction should be documented as part of the model specification.

Future research should extend the experiment using measured sub-hourly irradiance, site-specific PV modules, realistic load profiles, temperature-dependent battery models, degradation, multiple battery chemistries, and additional climate zones. A larger site sample would also permit stronger statistical inference and climate-stratified modeling. These extensions would improve absolute engineering accuracy while preserving the central methodological question established here: how much of a PV-battery reliability result is determined by the physical system, and how much is determined by the temporal representation of its weather input?.

ACKNOWLEDGMENTS

The author acknowledges NASA POWER for providing the openly accessible solar and meteorological resource data used in this study.

DATA AVAILABILITY

The six exact NASA POWER hourly CSV files used in the analysis are included in the accompanying empirical-study package. The package also contains the numerical tables, figures, data manifest, and reproduction script. The NASA POWER dataset is publicly accessible.

REFERENCES

[1] B. Y. H. Liu and R. C. Jordan, "The interrelationship and characteristic distribution of direct, diffuse and total solar radiation," *Solar Energy*, vol. 4, no. 3, pp. 1–19, 1960, doi: 10.1016/0038-092X(60)90062-1.

[2] D. G. Erbs, S. A. Klein, and J. A. Duffie, "Estimation of the diffuse radiation fraction for hourly, daily and monthly-average global radiation," *Solar Energy*, vol. 28, no. 4, pp. 293–302, 1982, doi: 10.1016/0038-092X(82)90302-4.

[3] D. R. Clark, S. A. Klein, and W. A. Beckman, "A method for estimating the performance of photovoltaic systems," *Solar Energy*, vol. 33, no. 6, pp. 551–555, 1984, doi: 10.1016/0038-092X(84)90010-0.

[4] T. Zhang, P. W. Stackhouse, Jr., W. S. Chandler, J. M. Hoell, D. Westberg, and C. H. Whitlock, "A global perspective on renewable energy resources: NASA's Prediction of Worldwide Energy Resources (POWER) Project," in *Proc. ISES World Congress 2007*, Beijing, China, 2007, vol. 4, pp. 2636 – 2640, doi: 10.1007/978-3-540-75997-3_532.

[5] T. Beck, H. Kondziella, G. Huard, and T. Bruckner, "Assessing the influence of the temporal resolution of electrical load and PV generation profiles on self-consumption and sizing of PV-battery systems," *Applied Energy*, vol. 173, pp. 331–342, 2016, doi: 10.1016/j.apenergy.2016.04.050.

[6] F. P. M. Kreuwel, W. H. Knap, L. R. Visser, W. G. J. H. M. van Sark, J. Vilà-Guerau de Arellano, and C. C. van Heerwaarden, "Analysis of high frequency photovoltaic solar energy fluctuations," *Solar Energy*, vol. 206, pp. 381–389, 2020, doi: 10.1016/j.solener.2020.05.093.

[7] A. Zurita, C. Mata-Torres, J. M. Cardemil, and R. A. Escobar, "Assessment of time resolution impact on the modeling of a hybrid CSP-PV plant: A case of study in Chile," *Solar Energy*, vol. 202, pp. 553–570, 2020, doi: 10.1016/j.solener.2020.03.100.

[8] I. Reda and A. Andreas, "Solar position algorithm for solar radiation applications," *Solar Energy*, vol. 76, no. 5, pp. 577–589, 2004, doi: 10.1016/j.solener.2003.12.003.

[9] R. Perez, R. Seals, P. Ineichen, R. Stewart, and D. Menicucci, "A new simplified version of the Perez diffuse irradiance model for tilted surfaces," *Solar Energy*, vol. 39, no. 3, pp. 221 – 231, 1987, doi: 10.1016/S0038-092X(87)80031-2.

[10] D. T. Reindl, W. A. Beckman, and J. A. Duffie, "Evaluation of hourly tilted surface radiation models," *Solar Energy*, vol. 45, no. 1, pp. 9–17, 1990, doi: 10.1016/0038-092X(90)90061-G.

[11] D. L. Evans, "Simplified method for predicting photovoltaic array output," *Solar Energy*, vol. 27, no. 6, pp. 555–560, 1981, doi: 10.1016/0038-092X(81)90051-7.

[12] D. L. King, W. E. Boyson, and J. A. Kratochvil, "Photovoltaic array performance model," *Sandia National Laboratories*, Albuquerque, NM, USA, Tech. Rep. SAND2004-3535, 2004, doi: 10.2172/919131.

[13] A. P. Dobos, PVWatts Version 5 Manual, NREL/TP-6A20-62641, *National Renewable Energy Laboratory*, Golden, CO, USA, 2014, doi: 10.2172/1158421.

[14] D. Faiman, "Assessing the outdoor operating temperature of photovoltaic modules," *Progress in Photovoltaics: Research and Applications*, vol. 16, no. 4, pp. 307–315, 2008, doi: 10.1002/pip.813.

[15] E. Skoplaki and J. A. Palyvos, "On the temperature dependence of photovoltaic module electrical performance: A review of efficiency/power correlations," *Solar Energy*, vol. 83, no. 5, pp. 614–624, 2009, doi: 10.1016/j.solener.2008.10.008.

[16] T. Huld, R. Müller, and A. Gambardella, "A new solar radiation database for estimating PV performance in Europe and Africa," *Solar Energy*, vol. 86, no. 6, pp. 1803 – 1815, 2012, doi: 10.1016/j.solener.2012.03.006.

[17] Y. Li, X. M. Chen, B. Y. Zhao, Z. G. Zhao, and R. Z. Wang, "Development of a PV performance model for power output simulation at minutely resolution," *Renewable Energy*, vol. 111, pp. 732–739, 2017, doi: 10.1016/j.renene.2017.04.049.

[18] R. Ayop, N. M. Isa, and C. W. Tan, "Components sizing of photovoltaic stand-alone system based on loss of power supply probability," *Renewable and Sustainable Energy Reviews*, vol. 81, pt. 2, pp. 2731–2743, 2018, doi: 10.1016/j.rser.2017.06.079.

[19] W. X. Shen, "Optimally sizing of solar array and battery in a standalone photovoltaic system in Malaysia," *Renewable Energy*, vol. 34, no. 1, pp. 348–352, 2009, doi: 10.1016/j.renene.2008.03.015.

[20] N. I. A. Aziz, S. I. Sulaiman, S. Shaari, I. Musirin, and K. Sopian, "Optimal sizing of stand-alone photovoltaic system by minimizing the loss of power supply probability," *Solar Energy*, vol. 150, pp. 220–228, 2017, doi: 10.1016/j.solener.2017.04.021.

[21] I. A. Ibrahim, T. Khatib, and A. Mohamed, "Impact of battery's model accuracy on size optimization process of a standalone photovoltaic system," *Sustainability*, vol. 8, no. 9, Art. no. 894, 2016, doi: 10.3390/su8090894.

[22] J. N. Ross, T. Markvart, and W. He, "Modelling battery charge regulation for a stand-alone photovoltaic system," *Solar Energy*, vol. 69, no. 3, pp. 181–190, 2000, doi: 10.1016/S0038-092X(00)00079-7.

[23] I. Sanz-Gorrachategui, C. Bernal, E. Oyarbide, E. Garayalde, I. Aizpuru, J. M. Canales, and A. Bono-Nuez, "New battery model considering thermal transport and partial charge stationary effects in photovoltaic off-grid applications," *Journal of Power Sources*, vol. 378, pp. 311 – 321, 2018, doi: 10.1016/j.jpowsour.2017.12.058.

[24] A. Degla, M. Chikh, A. Chouder, F. Bouchafaa, and A. Taallah, "Update battery model for photovoltaic application based on comparative analysis and parameter identification of lead-acid battery models behaviour," *IET Renewable Power Generation*, vol. 12, no. 4, pp. 484 – 493, 2018, doi: 10.1049/iet-rpg.2017.0409.

[25] J. Antonanzas, N. Osorio, R. Escobar, R. Urraca, F. J. Martinez-de-Pison, and F. Antonanzas-Torres, "Review of photovoltaic power forecasting," *Solar Energy*, vol. 136, pp. 78 – 111, 2016, doi: 10.1016/j.solener.2016.06.069.

[26] A. M. Elshurafa and M. H. Aldubyan, "State-of-charge effects on standalone solar-storage systems in hot climates: A case study in Saudi Arabia," *Sustainability*, vol. 11, no. 12, Art. no. 3471, 2019, doi: 10.3390/su11123471.

[27] M. Friedman, "The use of ranks to avoid the assumption of normality implicit in the analysis of variance," *Journal of the American Statistical Association*, vol. 32, no. 200, pp. 675 – 701, 1937, doi: 10.1080/01621459.1937.10503522.

[28] F. Wilcoxon, "Individual comparisons by ranking methods," *Biometrics Bulletin*, vol. 1, no. 6, pp. 80–83, 1945, doi: 10.2307/3001968.

[29] S. Holm, "A simple sequentially rejective multiple test procedure," *Scandinavian Journal of Statistics*, vol. 6, no. 2, pp. 65–70, 1979, doi: 10.2307/4615733.

[30] B. Efron, *The Jackknife, the Bootstrap and Other Resampling Plans*. Philadelphia, PA, USA: SIAM, 1982, doi: 10.1137/1.9781611970319.